Shahrood University of Technology

Journal of Mining and Environment (JME)

Journal homepage: www.jme.shahroodut.ac.ir

Iranian Society of Mining Engineering (IRSME)

Coupling Discontinuous Deformation Analysis and Displacement Discontinuity Method for Simulating Failure Mechanism in Geomaterials

Mohsen Khanizadeh Bahabadi[1]*, Alireza Yarahmadi Bafghi[1], Mohammad Fatehi Marji[1], Hosein Shahami[1], and Abolfazl Abdollahipour[2]

1. Faculty of Mining and Metallurgical, Department of Mine Exploitation Engineering, Yazd University, Yazd, Iran
2. School of Mining Engineering, College of Engineering, University of Tehran, Tehran, Iran

Article Info

Received 30 August 2023
Received in Revised form 17 December 2023
Accepted 30 December 2023
Published online 30 December 2023

DOI: 10.22044/jme.2023.13538.2502

Keywords

Geomaterials
Discontinuous deformation analysis
Displacement discontinuity method
Crack propagation
Coupled numerical methods

Abstract

Complexity of geomaterial's behavior is beyond the capabilities of conventional numerical methods alone for realistically model rock structures. Coupling of numerical methods can make the numerical modeling more realistic. Discontinuous Deformation Analysis (DDA) and Displacement Discontinuous Method (DDM) are hybridized for modeling block displacement and crack propagation mechanism in a blocky rock mass. DDA is used to compute the displacements of the blocks, and DDM is used to predict the crack propagation paths due to the specified boundary conditions. The displacements obtained from DDA are converted into stress and considering Kelvin's solution of the problem the crack propagation mechanism within each block is investigated. Boundary stresses are updated due to crack propagation and new stress boundary conditions in DDA. This cycle continued until crack propagation stopped or a new block formed. Numerical solutions of the experimental rock samples including two random cracks with crack 1 fixed and crack 2 created with different angles and one crack with a slope angle of 30 degrees are compared with the existing experimental and numerical results. This comparison validates the accuracy and effectiveness of the proposed procedure because crack propagation paths predicted are in good agreement with the corresponding experimental results of rock samples.

1. Introduction

Rock masses are mostly anisotropic, heterogeneous, and brittle materials associated with discontinuities in nature [1]. The main discontinuities in rock formations include fractures and weak planes such as defects, fissures, joints, faults, and bedding planes. They are formed by a wide range of geological processes due to the low tensile and shear strengths of rock mass, and relatively higher fluid conductivity compared to that of intact rock [2]. Rock joints are associated with intact rock bridges, which affect their persistency and interrupt the continuity of joints. The rock mass strength and stability in rock structures are significantly affected by rock bridges. Numerical methods for the analysis of rock materials are usually based on displacement and stress analysis. Generally, they are classified into three methods; boundary element method includes an indirect boundary element method such as a displacement discontinuity method (DDM) and a direct boundary element method [3], a finite difference method [4], and a finite element method [5]. Many mechanical and structural problems including fracture mechanics, heterogeneity and functionally graded layers are solved in literature using the analytical and numerical solutions [6-8].

For displacement and stress analysis in jointed rock masses, discrete element methods are used, which are usually classified into the following two categories: (a) the implicit method such as the

✉ *Corresponding author: m_khani_bahabadi@yahoo.com (M. Khanizadeh Bahabadi)*

discontinuous deformation analysis (DDA) [9-10], and (b) the explicit methods such as those used in the Itasca codes, e.g. PFC2D, PFC3D, UDEC, and 3DEC [11-13]. If the rock mass contains a large number of discontinuities or the conditions are complex, it is impossible to use analytical methods. Considering the development of computers, the complex conditions of the rock mass can be modeled using the capability of each of the numerical methods.

The DDA numerical method for modeling the dynamic behavior of discontinuities and blocky systems was first proposed by Shi, which is widely used in rock engineering problems such as masonry structures stability analysis, rock slope stability, dynamic wave propagation and blasting, and deep underground excavations, modeling of hydraulic fracture. The DDA method like the finite element method uses the principle of minimizing the total potential energy to obtain the equilibrium equations, and the displacements of the center of the block are the unknowns of the simultaneous equations [14].

Many researchers applied some changes to the original code provided by Shi to solve some problems in the DDA including crack propagation modeling capability. For example, Ke [15-16] pointed out that parameters such as fracture initiation, stress and strain distribution in the fracture process, crack propagation angle, energy reduction in the fracture process, and rock behavior in the presence of a joint should be considered for fracture simulation. He proposed a DDA code using 'artificial' joints for numerically simulating fracture propagation. Also, DDA with 'artificial' joints was used by Chiou et al. [17] to model the masonry structures. Chang [18] used a finite element mesh inside the DDA blocks to model the cantilever beam, but the results are qualitative. Clatworthy and Scheele [19] suggested sub-meshing to enhance block deformability. Koo and Chern [20] proposed an algorithm for modeling fracture blocks based on principal stresses which enables the gradual failure of blocks in the simulation process. They modeled the rock mass failure considering both tensile (mode 1) and shear (mode 2) failure modes. Amadi et al. [21-22] proposed the concept of sub-blocking in order to create the ability to block fracturing. These initial developments led to the coupling between DDA and FEM.

Ma et al. [23] proposed a Moving Least Squares (MLS) approximation for modeling crack propagation inside blocks and block failure in a similar way to DDA coupling with the Element Free Galerkin (EFG) method. Bao and Zhao [24-26] used the nodal-based DDA method for failure analysis, which has also been investigated by other researchers. Recently, Wang et al. [27] modeled the crack propagation mechanism by modifying the generalized maximum tangential stress criterion and using J-integrals (J_1 and J_2 integrals).

The DDM numerical method has been developed to simulate crack propagation in brittle materials. Three important failure initiation criteria have been proposed to study the crack propagation mechanism of brittle materials: (a) the maximum energy release rate (G-criterion), (b) the minimum energy density criterion (S-criterion), and (c) the maximum tangential stress (σ_θ-criterion) [28- 31]. In this study, the maximum tangential stress criteria in the DDM were used to investigate crack propagation.

The aim of this article is the simulation of rock failure mechanism in jointed rock masses considering the effects of rock bridges by coupling the DDA and the DDM. The DDA is used to determine the displacement of the block system due to the updated boundary stresses in each cycle of crack propagation, and the DDM is used to determine the crack propagation path due to the stresses resulting from the displacement in the DDA.

2. Methodology

Due to the presence of rock bridges in the rock mass and its effect on rock failure because of crack propagation caused by boundary displacement, simultaneous modeling of block system displacement and crack propagation caused by this displacement is required. Therefore, the DDA proposed by Shi has been used to model the displacement of the block system and the DDM proposed by Crouch [32] for the solution of elastostatic problems in solid mechanics has been used to model the crack propagation.

2-1- Discontinuity deformation analysis (DDA)

The DDA is a fundamental discontinuity method that is suitable for modeling large displacements. In the initial formulation of the DDA, the first-order displacement approximation is used, which makes the stress and strain constant in each block. The displacement (u, v) of each point (x, y) of each block can be represented by six displacement variables $(u_0, v_0, r_0, \varepsilon_x, \varepsilon_y, \gamma_{xy})$ (Figure 1), where (u_0, v_0) is the vertical and horizontal displacement of the specified point (x_0, y_0) in the block, r_0 is the rotation angle of the

block with the center of rotation (x_0, y_0) in radians and $\varepsilon_x, \varepsilon_y, \gamma_{xy}$ are the normal and shear strains of the block [33].

Equation 1 can be used to calculate the vertical and horizontal displacement at any point inside the block or on the block boundary when the displacements and strains of the center of the block are calculated. It should be noted that in the DDA formulation, the center of rotation with the (x_0, y_0) coordinate corresponds to the center of the block.

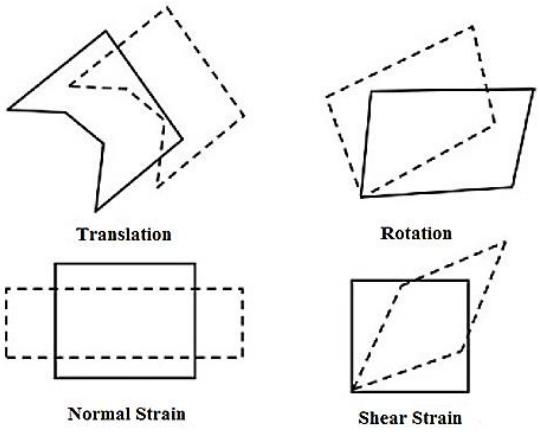

Figure 1. Displacement variables of DDA [33].

$$\begin{pmatrix} u \\ v \end{pmatrix} = \begin{pmatrix} 1 & 0 & -(y-y_0) & (x-x_0) & 0 & \frac{(y-y_0)}{2} \\ 0 & 1 & (x-x_0) & 0 & (y-y_0) & \frac{(x-x_0)}{2} \end{pmatrix} \begin{pmatrix} u_0 \\ v_0 \\ r_0 \\ \varepsilon_x \\ \varepsilon_y \\ \gamma_{xy} \end{pmatrix} \quad (1)$$

After calculating the horizontal and vertical displacement (u, v) on the block boundary, in order to convert these displacements into stress to be used as boundary stress in the DDM method, Kelvin's solution can be used [34]. The stresses for the plane strain version of Kelvin's solution are:

$$\begin{aligned} \sigma_{xx} &= F_x\left[2(1-\nu)g_{,x} - xg_{,xx}\right] + F_y[2\nu g_{,y} - yg_{,xx}] \\ \sigma_{yy} &= F_x\left[2\upsilon g_{,x} - xg_{,yy}\right] + F_y[2(1-\nu)g_{,y} - yg_{,yy}] \\ \sigma_{xy} &= F_x\left[(1-2\nu)g_{,y} - xg_{,xy}\right] + F_y[(1-2\nu)g_{,x} - yg_{,xy}] \end{aligned} \quad (2)$$

where F_x and F_y are the force in the X direction and the force in the Y direction, respectively, and ν is the Poisson's ratio. The derivatives of the function $g(x, y)$ in the above expressions are found directly from (3).

$$g(x,y) = \frac{-1}{4\pi(1-\upsilon)} ln(x^2 + y^2)^{\frac{1}{2}} \quad (3)$$

To use Kelvin's solution, first, according to Equation 4, the boundary displacements calculated from the DDA are converted into horizontal and vertical forces.

$$\begin{aligned} F_x &= K * u \\ F_y &= K * v \end{aligned} \quad (4)$$

where K is the stiffness of the spring, and (u, v) are displacement in horizontal and vertical directions, respectively.

2.2. Displacement discontinuity method (DDM)

A displacement discontinuity method (DDM) is an indirect boundary element method for the solution of elastostatic problems in solid mechanics that was originally proposed by Crouch [34]. This method is very practical and appropriate for modeling crack propagation problems in rock fracture mechanics. In this method, the amount of deformation normal and parallel to the crack (deformation caused by crack opening and deformation caused by crack sliding) can be easily calculated. In this article, displacement discontinuity elements with a higher order (quadratic elements, i.e., elements that are of order two and have three sub-elements) are used to achieve high accuracy in discontinuity displacements. A displacement discontinuity element of length 2c on the x-axis is shown in Figure 2(a), and the widespread displacement

discontinuity variable $u(\zeta)$ can be calculated. By taking the u_x and u_y components of the general displacement discontinuity $u(\zeta)$ in the interval (-c +c), as shown in Figure 2(b); D_x and D_y are easily determined. The displacement discontinuity element surfaces can be distinguished into a positive side of y ($y = 0_+$) and a negative side of y ($y = 0_-$) [35].

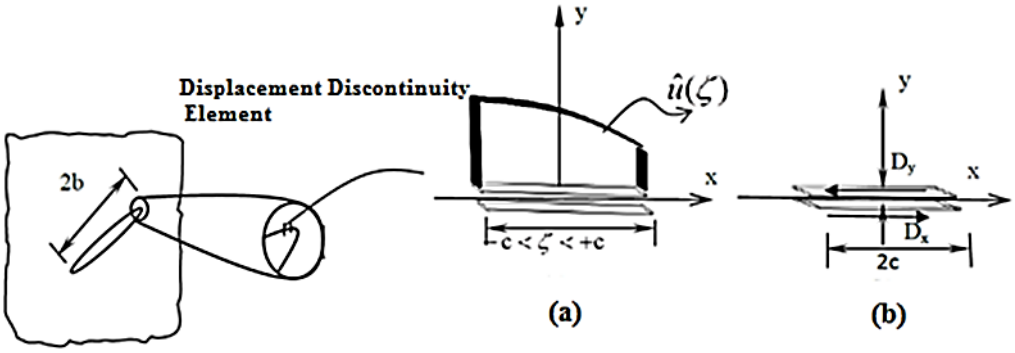

Figure 2. (a) Displacement discontinuity element and widespread displacement discontinuity variable $u(\zeta)$, (b) constant element displacement discontinuity [35].

Therefore, the constant element displacement discontinuities D_x and D_y can be written as:

$$D_x = u_x(x, 0_-) - u_x(x, 0_+), \quad D_y = u_y(x, 0_-) - u_y(x, 0_+) \tag{5}$$

The positive sign convention of D_x and D_y is shown in Figure 2(b), and demonstrates that when the two surfaces of the displacement discontinuity overlap D_y is positive, it leads to a physically impossible situation. This conceptual difficulty is overcome by considering that the element has a finite thickness, in its undeformed state which is small compared to its length, but bigger than D_y [36].

The quadratic element displacement discontinuity is based on the analytical integration of quadratic collocation shape functions over collinear, straight-line displacement discontinuity elements. Figure 3 shows the displacement distributions at the quadratic collocation point 'n', which can be written in a general form as:

$$D_j(\zeta) = N_1(\zeta)D_j^1 + N_2(\zeta)D_j^2 + N_3(\zeta)D_j^3 \tag{6}$$

$$j = x, y$$

where D_j^1, D_j^2, and D_j^3 are the quadratic nodal displacement discontinuities, and

$$N_1(\zeta) = \frac{\zeta(\zeta - 2c_1)}{8c_1^2}$$

$$N_2(\zeta) = \frac{-(\zeta^2 - 4c_1^2)}{4c_1^2} \tag{7}$$

$$N_3(\zeta) = \frac{\zeta(\zeta + 2c_1)}{8c_1^2}$$

are the quadratic collocation shape functions using $c_1 = c_2 = c_3$. A quadratic element has three nodes, which are at the centers of its three sub-elements (see Figure 3) [35].

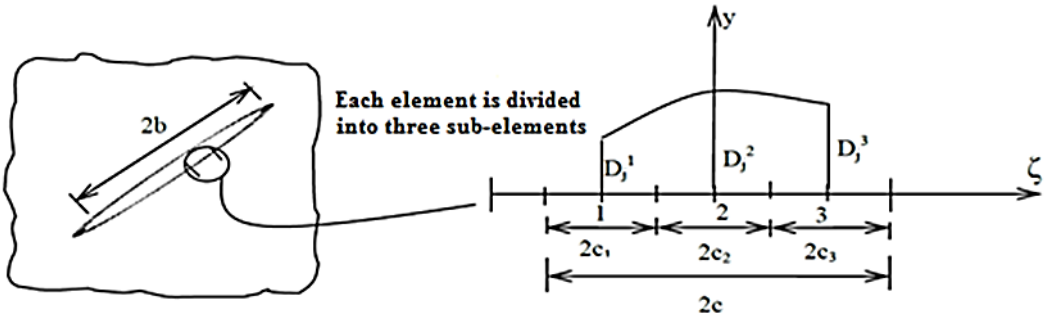

Figure 3. Quadratic collocations for higher order displacement discontinuity variation [35].

The displacements and stresses for a line crack in an infinite body along the x-axis, in terms of single harmonic functions g(x,y) and f(x,y), are given by Crouch and Starfield (1983) as:

$$u_x = \left[2(1-\upsilon)f_{,y} - yf_{,xx}\right] + \left[-(1-2\upsilon)g_{,x} - yg_{,xy}\right]$$
$$u_y = \left[(1-2\upsilon)f_{,x} - yf_{,xy}\right] + \left[2(1-\upsilon)g_{,y} - yg_{,yy}\right] \quad (8)$$

and the stresses are:

$$\sigma_{xx} = 2\mu\left[2f_{,xy} + yf_{,xyy}\right] + 2\mu\left[g_{,yy} + yg_{,yyy}\right]$$
$$\sigma_{yy} = 2\mu\left[-yf_{,xyy}\right] + 2\mu\left[g_{,yy} - yg_{,yyy}\right] \quad (9)$$
$$\sigma_{xy} = 2\mu\left[2f_{,yy} + yf_{,yyy}\right] + 2\mu\left[-yg_{,xyy}\right]$$

where μ is shear modulus, and $f_{,x}$, $g_{,x}$, $f_{,y}$, $g_{,y}$, etc. are the partial derivatives of the single harmonic functions f(x, y) and g(x,y) with respect to x and y. These potential functions (for a quadratic variation of displacement discontinuity along the element) can be found from:

$$f(x,y) = \frac{-1}{4\pi(1-\upsilon)}\sum_{j=1}^{3} D_x^j F_j(I_0, I_1, I_2)$$
$$g(x,y) = \frac{-1}{4\pi(1-\upsilon)}\sum_{j=1}^{3} D_y^j F_j(I_0, I_1, I_2) \quad (10)$$

The common function F_j, is defined as:

$$F_j(I_0, I_1, I_2) = \int N_j(\zeta) ln[(x-\zeta) + y^2]^{\frac{1}{2}} d\zeta, \quad (11)$$
$$j = 1 - 3$$

The integrals I_0, and I_1 and I_2 are expressed as:

$$I_0(x,y) = \int_{-c}^{c} ln[(x-\zeta)^2 + y^2]^{\frac{1}{2}} d\zeta = y(\theta_1 - \theta_2) - (x-c)\, ln(r_1) + (x+c)\, ln(r_2) - 2c \quad (12\text{-a})$$

$$I_1(x,y) = \int_{-c}^{c} \varepsilon ln[(x-\zeta)^2 + y^2]^{\frac{1}{2}} d\zeta = xy(\theta_1 - \theta_2) + 0.5(y^2 - x^2 + c^2)\, ln\left(\frac{r_1}{r_2}\right) - cx \quad (12\text{-b})$$

$$I_2(x,y) = \int_{-c}^{c} \varepsilon^2 ln[(x-\zeta)^2 + y^2]^{\frac{1}{2}} d\zeta =$$
$$\frac{y}{3}(3x^2 - y^2)(\theta_1 - \theta_2) + \frac{1}{3}(3xy^2 - x^3 + c^3)\, ln(r_1) - \frac{1}{3}(3xy^2 - x^3 + c^3)\, ln(r_2) - \frac{2c}{3}(x^2 - y^2 + \frac{c^2}{3}) \quad (12\text{-c})$$

where the terms θ_1, θ_2, r_1, and r_2 are defined as:

$$\theta_1 = arctan\left(\frac{y}{x-c}\right)$$
$$\theta_2 = arctan\left(\frac{y}{x+c}\right)$$
$$r_1 = [(x-c)^2 + y^2]^{\frac{1}{2}} \quad (13)$$
$$r_2 = [(x+c)^2 + y^2]^{\frac{1}{2}}$$

In order to eliminate the singularity of stress and displacement calculations near the crack tip and increase the accuracy of DDM near the crack tip, as shown in Figure 4, by using a special crack tip element with the length of 2c, the displacement discontinuity variations along this element can be written as the following form:

$$D_j(\zeta) = A_{T1}(\zeta)D_j^1 + A_{T2}(\zeta)D_j^2 + A_{T3}(\zeta)D_j^3$$
$$j = x, y \quad (14)$$

The shape functions A_{T1}, A_{T2}, and A_{T3} can be calculated according to Equation 15.

$$A_{T1}(\zeta) = \frac{15\zeta^{\frac{1}{2}}}{8c_1^{\frac{1}{2}}} - \frac{\zeta^{\frac{3}{2}}}{c_1^{\frac{3}{2}}} + \frac{\zeta^{\frac{5}{2}}}{8c_1^{\frac{5}{2}}}$$
$$A_{T2}(\zeta) = \frac{-5\zeta^{\frac{1}{2}}}{4\sqrt{3}c_1^{\frac{1}{2}}} + 3\frac{\zeta^{\frac{3}{2}}}{2\sqrt{3}c_1^{\frac{3}{2}}} - \frac{\zeta^{\frac{5}{2}}}{4\sqrt{3}c_1^{\frac{5}{2}}} \quad (15)$$

$$A_{T3}(\zeta)=\frac{3\zeta^{\frac{1}{2}}}{8\sqrt{5}c_1^{\frac{1}{2}}}-\frac{\zeta^{\frac{3}{2}}}{2\sqrt{5}c_1^{\frac{3}{2}}}+\frac{\zeta^{\frac{5}{2}}}{8\sqrt{5}c_1^{\frac{5}{2}}}$$

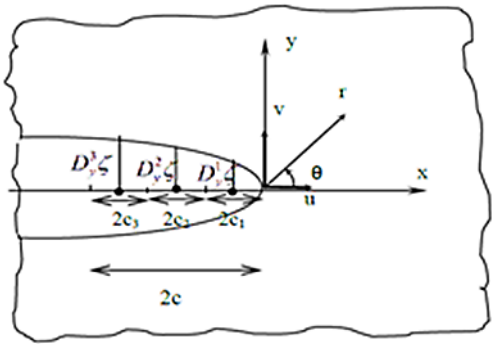

Figure 4. A special crack tip element with three equal sub-elements [35].

Based on the LEFM theory, the Mode I and Mode II stress intensity factors K_I and K_{II} can be written in terms of the normal and shear displacement discontinuities as [36]:

$$K_I=\frac{\mu}{4(1-\upsilon)}\left(\frac{2\pi}{c}\right)^{\frac{1}{2}}D_y(c)$$
$$K_{II}=\frac{\mu}{4(1-\upsilon)}\left(\frac{2\pi}{c}\right)^{\frac{1}{2}}D_x(c) \quad (16)$$

2.3. Coupling of DDA and DDM methods

Generally, in rock mechanics and porous media making a coupling between two physics or two different numerical methods is really complex due to the complexity of the equations and programming algorithms [37-39]. Although the mentioned couplings are very complicated, in this article, an attempt is made to establish a coupling between the two methods DDM and DDA. In fact, this article uses the DDM method to simulate crack propagation and the DDA method to simulate displacement. For modeling crack propagation simultaneously with displacements due to the initial stress state in block systems, firstly, the DDA method is employed to establish the numerical model and for the initial solution of the problem. The displacements calculated from DDA are converted into boundary stresses by using Kelvin's problem, and then they are used as boundary conditions in the DDM method, and stress intensity factors and crack growth angles are calculated. The boundary stresses caused by crack propagation are updated and applied as stresses on the boundary in the DDA method, and the displacement caused by the new stresses is calculated. This cycle will continue until the crack growth stops, and if a new block is formed, the geometric model will be updated. Figure 5 illustrates the process of calculating crack propagation by a couple of DDA and DDM methods.

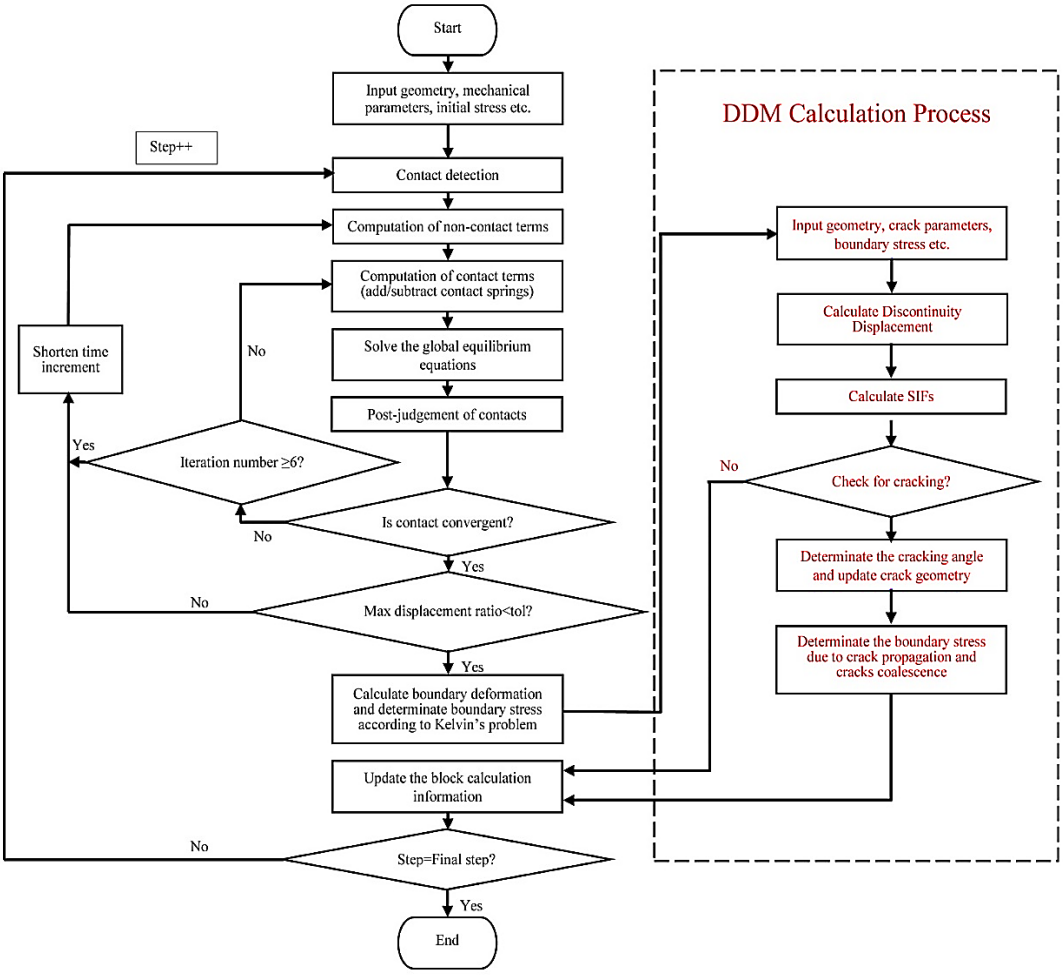

Figure 5. The flow chart couple of DDA and DDM methods.

3. Numerical Simulation

A coupling between DDA and DDM methods is verified herein for the simulation of close crack propagation. The simulation results of crack propagation were analyzed and compared with the experimental tests of Haeri et al. [40] and a study of the failure process in brittle rocks containing pre-existing flaws under uniaxial compression has been conducted by Wong et al. [41-43]. In these experimental studies, differences in the patterns of cracks created under compressive stress have been seen, which depend on the materials used and crack angle.

3.1. Numerical simulation of sample with double cracks

Haeri et al. [40] investigated a series of experiments on the samples containing 2 random cracks 1 and 2. Figure 6 depicts the geometry and loading conditions of rock-like samples consisting of pozzolana Portland cement, fine sand, and water. The diameter and length of the used samples are 60 and 120 mm, respectively. The specimen was loaded with the vertical load. The mechanical characteristics of rock-like samples without cracks (intact) are given in Table 1 [40].

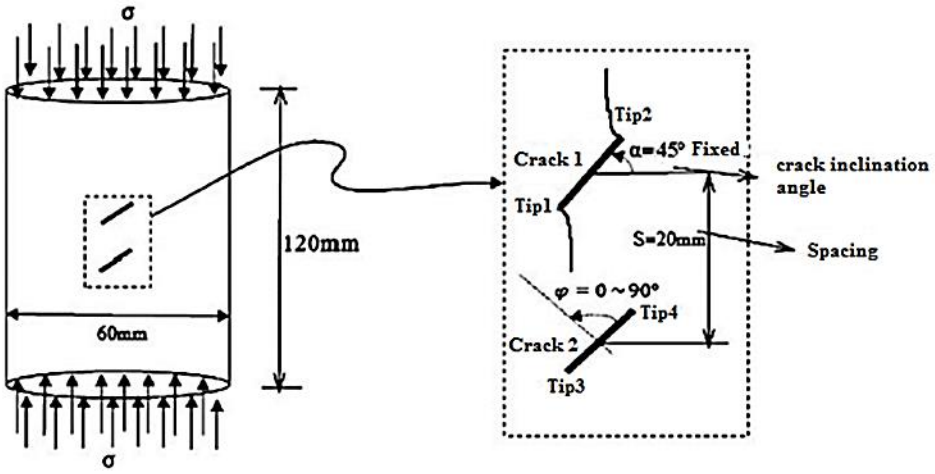

Figure 6. Geometry of rock-like sample under uniaxial pressure [40].

Table 1. Mechanical properties of the rock-like specimens [40].

Characteristic	Value
Uniaxial compression strength (MPa)	28
Modulus of elasticity (GPa)	17
Poisson's ratio	0.21
Fracture toughness (MPa.$m^{\frac{1}{2}}$)	2

Uniaxial compression tests have been performed on samples containing 2 random cracks 1 and 2 with lengths 2b = 10 mm. In these samples, crack 1 is fixed with a slope angle of 45 degrees, and the slope of crack 2 is created with different angles of 0, 30, 60, and 90 degrees, as schematically shown in Figure 7. The uniaxial compressive stress σ is uniformly applied at a constant rate of 0.2 MPa/s. Also, the locations of these 2 cracks are determined by the position of the crack tips, that is tip 1, tip 2, tip 3, and tip 4, respectively.

The calculation parameters of the DDA method are as follows: the time step was set at 1s, the maximum displacement ratio was 0.001, and the stiffness of the contact between the blocks was 200 GPa.

Figures 8a-d show the simulation results of crack propagation of the four different specimens already shown in Figures 7a–d by the proposed numerical method. According to the comparison shown in Figures 9a-d between the proposed numerical method results in this paper, experimental results, and numerical results obtained by the boundary element simulation [40], the simulation data match the experimental, and DDM simulation results.

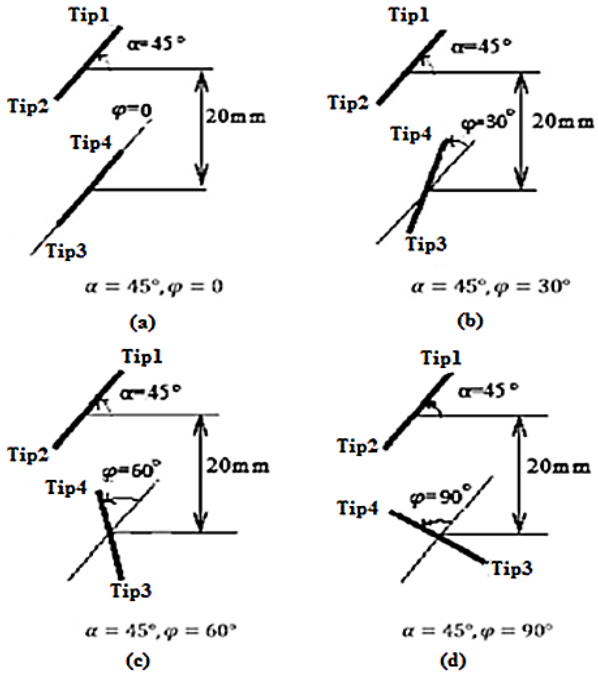

Figure 7. Crack geometries with spacing S = 20 mm [40].

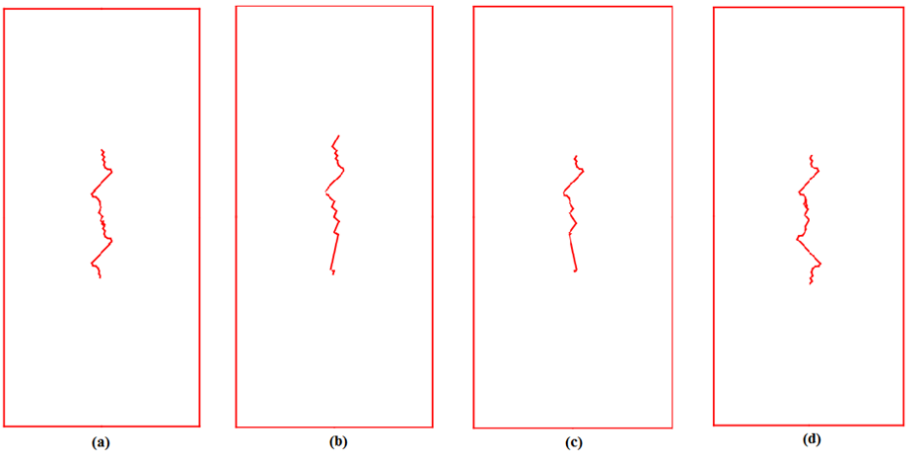

Figure 8. Proposed numerical method results illustrating the coalescence path of rock-like specimens containing two cracks: (a) $\alpha = 45^{\circ}, \varphi = 0$; (b) $45^{\circ}, \varphi = 30^{\circ}$; (c) $45^{\circ}, \varphi = 60^{\circ}$; (d) $45^{\circ}, \varphi = 90^{\circ}$.

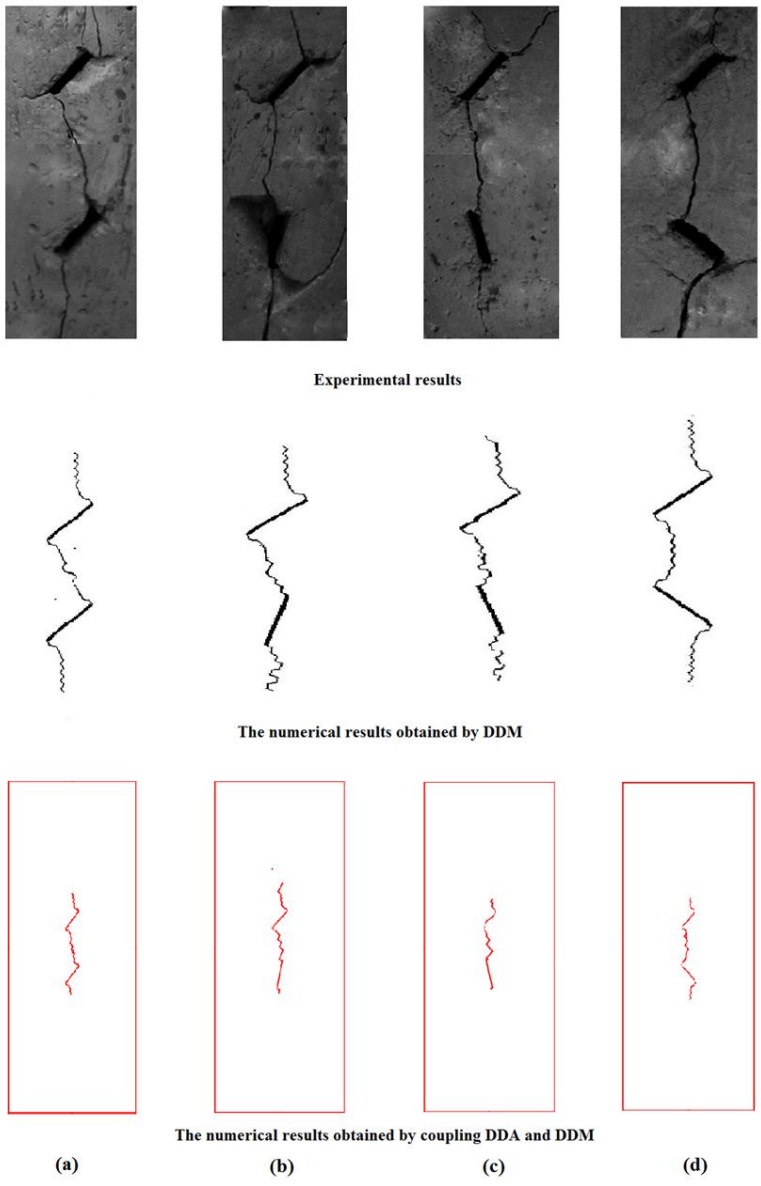

Figure 9. Comparison between experimental results and proposed numerical results obtained by DDM illustrating the coalescence path of rock-like specimens containing two cracks: (a) $\alpha = 45^{\circ}, \varphi = 0$; (b) $45^{\circ}, \varphi = 30^{\circ}$; (c) $45^{\circ}, \varphi = 60^{\circ}$; (d) $45^{\circ}, \varphi = 90^{\circ}$.

3.2. Numerical simulation of sample with single crack

Wong et al. [41] numerically presented the solution for the compression test on the rock-like specimens with a single random crack by using a finite element code, which one of the mentioned cases is simulated herein. Figure 10 illustrates the geometry and loading conditions of the specimen. The length and width of the specimen containing a center slant flaw with a half-length b =10 mm and inclination angle of 30 degrees are 170 mm and 50 mm, respectively. The mechanical parameters of the specimen used in the simulation are presented in Table 2.

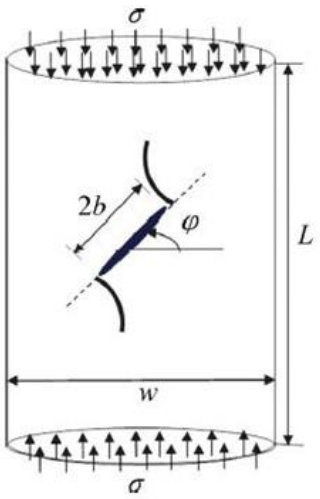

Figure 10. The geometry and loadingconditions of the test specimen [44].

Table 2. Mechanical properties of the rock-like specimen [44].

Characteristic	Value
Uniaxial compression strength (MPa)	200
Modulus of elasticity (GPa)	50
Poisson's ratio	0.25
Fracture toughness (MPa.$m^{\frac{1}{2}}$)	1.2

The numerical results obtained by coupling the DDA and DDM method are shown in Figure 11. For this example, Wong et al. [41] used the $RFPA^{2D}$ (a 2D finite element code) to conduct numerical simulation, and Haeri et al. [44] used the indirect boundary element method for numerical simulation. Figure 12. demonstrates that the simulation results obtained from the coupling DDA and DDM method are in good agreement with the finite element code and indirect boundary element method results.

Figure 11. Proposed numerical method simulation of crack propagation process in pre-cracked specimen with crack inclination angle 30 degrees.

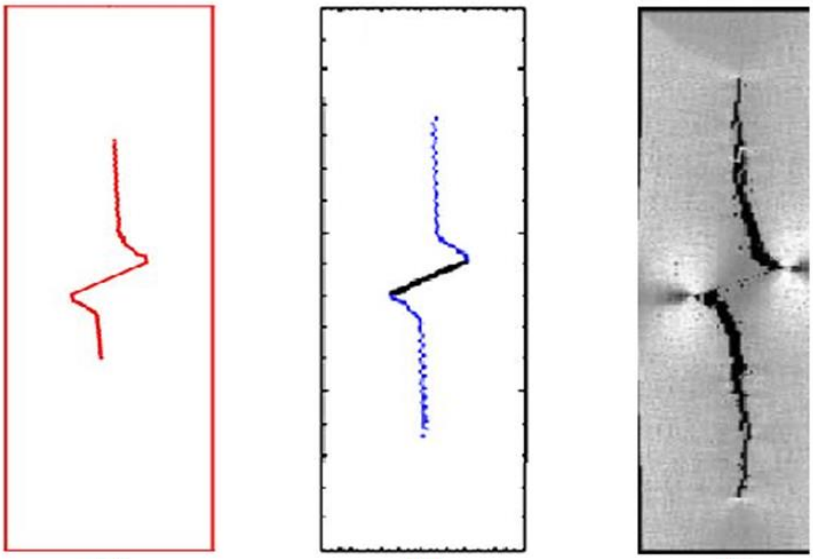

Figure 12. (a) Result of coupling between DDA and DDM method, (b) Indirect boundary method result of Haeri et al. [44], and (c) A finite element code result (RFPA^{2D}) of Wong et al. [41] of crack propagation process in pre-cracked specimen with crack inclination angle 30 degrees.

3. Simulation Results

The uniaxial compression of the specimens with a single center crack and double cracks are simulated by the coupling of DDA and DDM methods, and the simulation data is compared with the experimental and numerical results. Figure 9 depicts the comparison between the proposed numerical method, experimental and indirect boundary element method results for the case, where crack 1 is fixed with a slope angle of 45 degrees and the slope of crack 2 is created with different angles of 0, 30, 60, and 90 degrees. All of the proposed numerical method simulation data agreed with the experimental findings and DDM simulation data.

Figure 13 compares the simulation data by two numerical methods with the experimental results in detail. The black line represents the crack propagation path obtained from the experimental result and DDM simulation result, while the red line represents the crack propagation path in coupling DDA and DDM method simulation results. The coupling between DDA and DDM simulation data agrees well with the experimental results and DDM simulation results.

In addition, the effect of the inclination angle of crack 2 compared to crack 1 is analyzed, and the comparison results are listed in Table 3. The difference between the coupling DDA and DDM simulation data, experimental data, and DDM simulation data is minimal, confirming that the proposed numerical method can effectively simulate crack propagation.

Table 3. The comparison of equation of the line coalescence of cracks propagating from the tips of pre-existing cracks in numerical methods and experimental data

Crack inclination angle		Line equation			Propagation angle (degree)		
Crack 1	Crack 2	Experimental	Proposed numerical	DDM method	Experimental	Proposed numerical	DDM method
$\alpha = 45^{\circ}$	$\varphi = 0^{\circ}$	y = -2.2476x + 0.1397	y = -2.6289x + 0.15	y = -2.0251x + 0.1291	-66.01	-69.17	-63.72
	$\varphi = 30^{\circ}$	y = 0.4046x + 0.0545	y = -2.6167x + 0.1356	y = -2.2349x + 0.1275	22.03	-69.08	-65.89
	$\varphi = 60^{\circ}$	y = -4.5152x + 0.1693	y = -2.4787x + 0.1257	y = -2.7013x + 0.1277	-77.51	-68.03	-69.68
	$\varphi = 90^{\circ}$	y = 0.0178x + 0.0294	y = 0.0043x + 0.0302	y = -0.0059x + 0.0323	1.02	0.25	-0.33

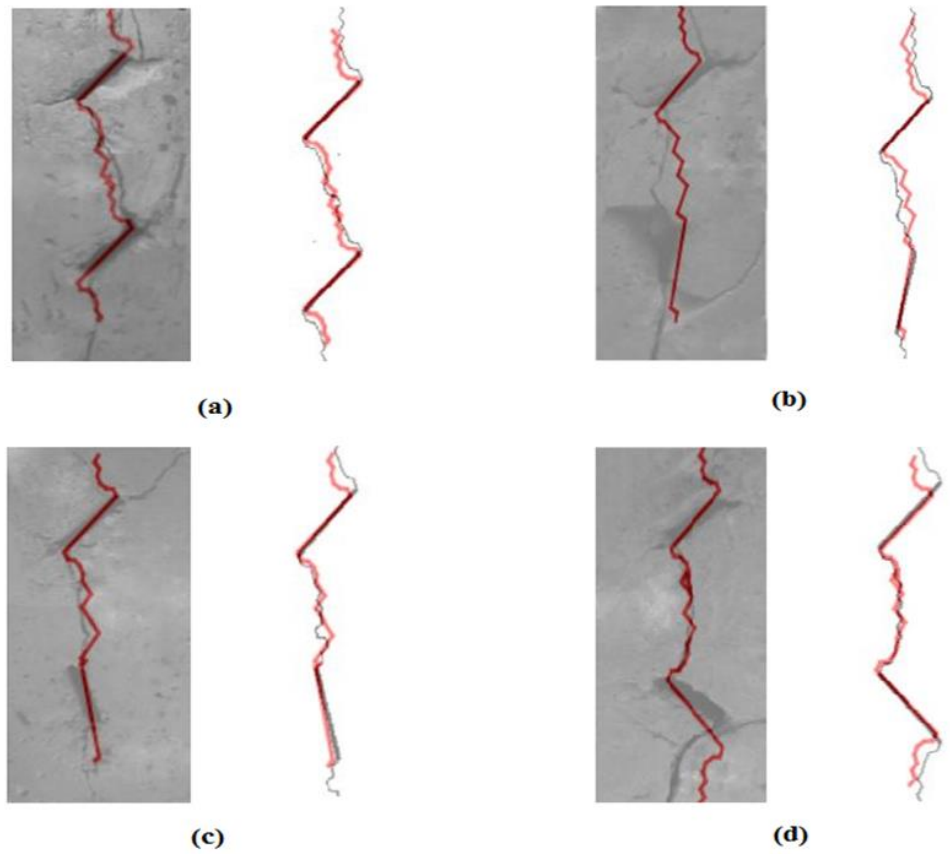

Figure 13. Qualitative examination of the compatibility of the results of the experimental method and the DDM numerical method with the results of the coupled DDA and DDM method in the rock-like specimens containing two cracks: (a) $\alpha = 45^{\circ}, \varphi = 0$; (b) $45^{\circ}, \varphi = 30^{\circ}$; (c) $45^{\circ}, \varphi = 60^{\circ}$; (d) $45^{\circ}, \varphi = 90^{\circ}$.

Figure 14 shows the comparison of crack propagation results in the sample with a single crack under compression test by three numerical methods: indirect boundary method, finite element code (RFPA$^{2D)}$ and coupling DDA, and DDM method. According to this figure, the coupling DDA and DDM simulation data agrees well with the RFPA^{2D} results and DDM simulation results.

One of the most important and influential parameters in the crack propagation process is its growth angle, which depends on the values of the stress intensity factors (KI and KII) and the crack inclination angle. In the numerical process of coalescence, the cracks step by step, in each step, the values of the stress intensity factors and the starting angle of wing cracks have been calculated. At this stage, the crack expansion from each pre-existing crack tip is developed by 1 mm to 2 mm and joins together at a point between the rock bridges. The numerical values of the stress intensity factors for the 4 samples introduced in Figure 7, in the first step of the crack propagation process, are given in Table 4.

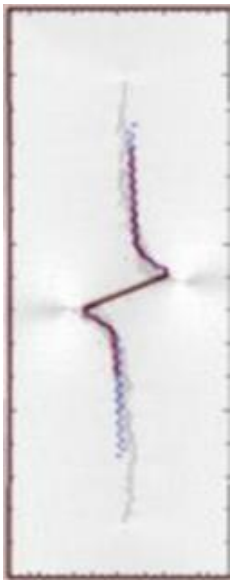

Figure 14. Qualitative examination of the compatibility of the results of the RFPA^{2D} method and the DDM numerical method with the results of the coupled DDA and DDM method in the rock-like specimens containing a single crack.

Table 4. Numerical Values of *KI* and *KII* for the four crack tips of two pre-existing cracks.

Crack inclination angle		*KI*				*KII*			
Crack 1	**Crack 2**	**Tip 1**	**Tip 2**	**Tip 3**	**Tip 4**	**Tip 1**	**Tip 2**	**Tip 3**	**Tip 4**
$\alpha = 45^{\circ}$	$\varphi = 0^{\circ}$	0.7446	0.653886	0.676481	0.70628	0.754628	0.643411	0.613789	0.67096
	$\varphi = 30^{\circ}$	0.78038	0.710145	0	0	0.75525	0.675427	0.717474	0.655737
	$\varphi = 60^{\circ}$	1.12938	1.04679	0	0	1.06537	0.929959	0.723031	0.664009
	$\varphi = 90^{\circ}$	0.72371	0.64487	0.816449	0.726444	0.712308	0.565902	0.794558	0.631245

Figure 15 shows the numerical results of crack initiation and coalescence stresses. The numerical values of wing crack initiation stresses for the 4 introduced samples are around 2.24-5.23 MPa, and the experimental values of wing crack initiation stresses are around 6.8-12.7 MPa. On the other hand, the coalescence stresses of the numerical cracks are around 13.2-16.8 MPa, and the stress of the initiation of experimental wing cracks is around 17.8-20.3 MPa.

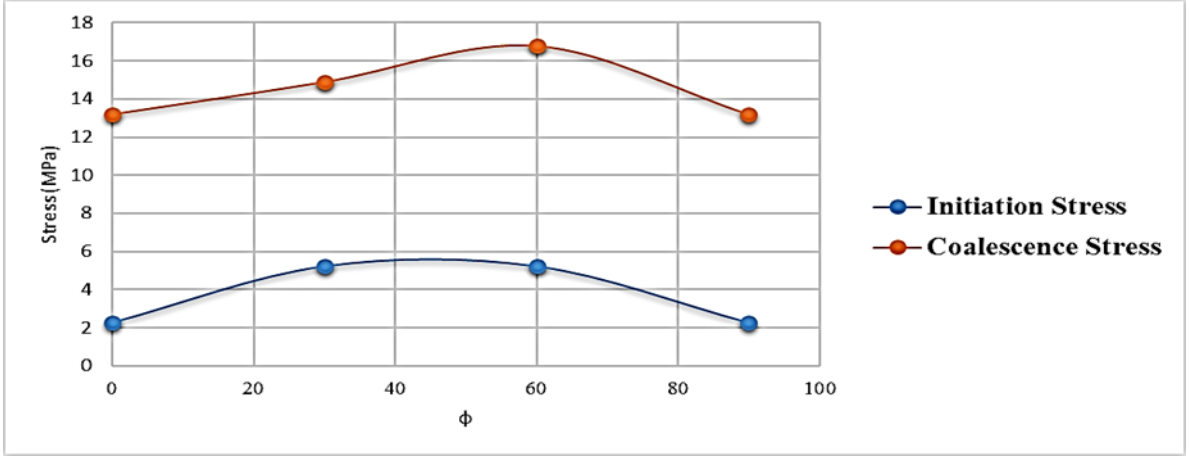

Figure 15. Stresses of crack initiation and coalescence process versus different angles of crack 2 with respect to the direction of crack 1 (φ =0, 30, 60, and 90) in the proposed numerical method.

The ratios of final breakage stress to the uniaxial compressive strength ($\frac{\sigma_F}{\sigma_C}$) for the four cases $\varphi = 0$, 30, 60, and 90 are given in Figure 16. As shown in Figures 15 and 16, the stresses of the cracked specimens at different stages of the crack propagation process are increasing for $\varphi = 30^{\circ}$ and $\varphi = 60^{\circ}$ but decreasing for $\varphi = 0^{\circ}$ and $\varphi = 90^{\circ}$, respectively.

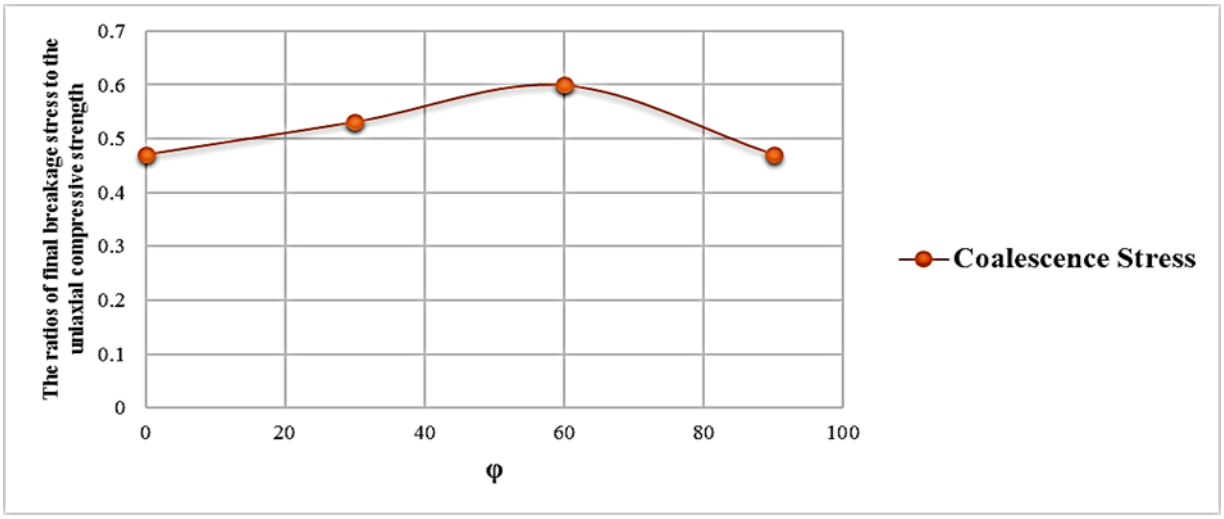

Figure 16. $\frac{\sigma_F}{\sigma_C}$ ratio versus different angles of crack 2 with respect to the direction of crack 1 (φ =0, 30, 60, and 90) in the proposed numerical method.

Since the coupling of discontinuous deformation analysis and discontinuity displacement method is used in this article, it is possible to calculate the strain values resulting from the crack initiation and coalescence process. Figure 17 shows the strain values obtained from the discontinuous deformation analysis method.

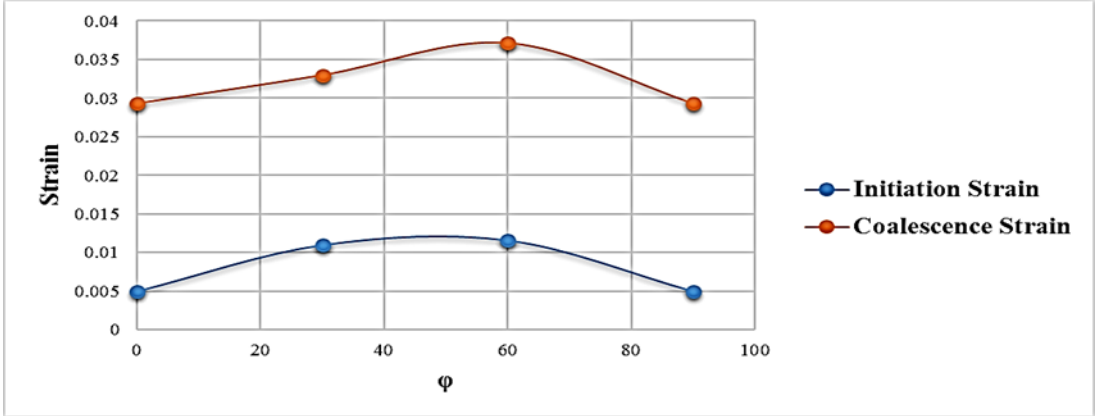

Figure 17. Strains of crack initiation and coalescence process versus different angles of crack 2 with respect to the direction of crack 1 (φ = 0, 30, 60, and 90).

4. Conclusions

The natural fractures and rock bridges in blocky rock masses affect the stability of engineering rock structures. In rock blocks, the crack initiation and coalescence phenomena depend on the rock bridges which may cause the formation of new blocks and create instability in rock slopes. The displacements that occur in the block system may lead to the growth of cracks in the rock bridges and join them to form new blocks. In this research work, the modeling of rock bridges and the way of crack propagation in the rock block are investigated numerically using the coupling methods. The following main conclusions are obtained:

In order to simultaneously model block displacement and crack propagation mechanism (in a rock block), discontinuous deformation analysis (DDA) and displacement discontinuity method (DDM) have been coupled.

In this approach, the displacements obtained from the DDA solution of the problem are converted into stress boundary conditions for each block, and then based on Kelvin's problem, the fundamental solution for each boundary element is evaluated using DDM.

The crack propagation mechanism is investigated using the higher-order (quadratic) displacement discontinuity elements in the DDA-DDM code.

The crack propagation paths that are affected by rock bridges and the boundary stresses are updated after each step and applied as new boundary conditions for the DDA solution.

The numerical and experimental modeling results of cracked rock samples under the uniaxial compression test are compared with one another.

The crack propagation angles and the crack coalescence paths of the two cracks in the experimental and modeled rock samples were in good agreement.

The results of this study showed the effect of stress ratio and orientation of the second crack on the paths of propagation and coalescence of the two cracks in the rock sample.

In this new method, it is also possible to calculate strain values at each stage of crack propagation.

This method can be used for the stability analysis of rock slopes considering the simultaneous effects of displacements and crack propagations resulting in a more accurate stability analysis of the rock structures.

References

[1]. Harrison, J. and Hudson, J. (2001). Engineering Rock Mechanics: Part 2: Illustrative Worked Examples. *Elsevier Science*.

[2]. Khan, M. (2010). Investigation of Discontinuous Deformation Analysis for Application in Jointed Rock Masses. *University of Toronto. Retrieved from http://hdl.handle.net/1807/24785*.

[3]. Alizadeh, R., Fatehi Marji, M., Abdollahipour, A., and Pourghasemi Sagand, M. (2023). Numerical simulation of fatigue crack propagation in heterogeneous geomaterials under varied loads using displacement discontinuity method. *Rock Mechanics and Geotechnical Engineering, 15(3), 702-716.*

[4]. Yang, W., Zhang, Q., P.G, R, Yu, R., Luo, G., Chenchen, H., and Wang, G. (2019). A damage mechanical model applied to analysis of mechanical properties of jointed rock masses. *Tunnelling and Underground Space Technology, 84, 113-128.*

[5]. Du, X., Pei, Z., Jin, L., and Lu, D. (2019). A multi-scale analysis method for the simulation of tunnel excavation in sandy cobble stratum. *Tunnelling and Underground Space Technology, 83, 220-230.*

[6]. Yaylacı, M., Abanoz, M., Yaylacı, E.U.(2022). Evaluation of the contact problem of functionally graded layer resting on rigid foundation pressed via rigid punch by analytical and numerical (FEM and MLP) methods. *Arch Appl Mech, 92, 1953–1971.*

[7]. Turan, M., Uzun Yaylacı, E., and Yaylacı, M. (2023). Free vibration and buckling of functionally graded porous beams using analytical, finite element, and artificial neural network methods. *Arch Appl Mech, 93, 1351–1372.*

[8]. Yaylaci, E. U., Oner, E., Yaylaci, M., Ozdemir, M. E., Abushattal, A., and Birinci, A. (2022). Application of artificial neural networks in the analysis of the continuous contact problem. *Structural Engineering and Mechanics, 84(1), 35–48.*

[9]. Shahami, M., Yarahmadi Bafghi, A., and Fatehi Marji, M. (2019). Investigating the effect of external forces on the displacement accuracy of discontinuous deformation analysis (DDA) method. *Computers and Geotechnics, 111, 313-323.*

[10]. Shahami, M., Yarahmadi Bafghi, A., and Fatehi, M. (2022). Key group analysis based on DDA method for rock slope stability analysis. *Analytical and Numerical Methods in Mining Engineering, 11(29), 17-25.*

[11]. Cundall, P. (2004). UDEC 4.0 manual-theory and background. *ITASCA Consulting Group. Retrieved from https://www.itascacg.com/software/udec*.

[12]. Lak, M., Fatehi Marji, M., Yarahamdi Bafghi, A., and Abdollahipour, A. (2019b). Discrete element modeling of explosion-induced fracture extension in jointed rock masses. *Mining and Environment, 10(1), 125-138.*

[13]. Group, I. C. (2008). PFC3D (Particle Flow Code in 3 Dimensions). *Version 4.0. Itasca Consulting Group Inc., Minneapolis. Retrieved from https://www.itascacg.com/software/PFC*.

[14]. Hatzor, Y., Ma, G., and Shi, G.h. (2017). Discontinuous Deformation Analysis in Rock Mechanics Practice (1st Edition ed.). *London: CRC Press.*

[15]. Ke, T.C. (1993). Simulated testing of two dimensional heterogeneous and discontinuous rock masses using discontinuous deformation analysis. *University of California, Berkeley*.

[16]. Ke, T.C. (1997). Application of DDA to simulate fracture propagation in solid. *In Proceedings of the Second International Conference on Analysis of Discontinuous Deformation, Ohnishi Y (ed.), 155-185*.

[17]. Chiou, Y., Tzeng, J., and Lin, M. (1995). Discontinuous deformation analysis for masonry structures. *In Proceedings of the First International Conference on Analysis of Discontinuous Deformation, Li J.C, Wang C.Y, Sheng J. (eds), 288-297*.

[18]. Chang, C. (1994). Nonlinear dynamic discontinuous deformation analysis with finite element meshed block system. *Ph.D. thesis, University of California, Berkeley*.

[19]. Clatworthy, D. and Scheele, F. (1999). A method of sub-meshing in discontinuous deformation analysis (DDA). *In ICADD-3: Third International Conference on Analysis of Discontinuous Deformation From, Theory to Practice, Amadei B (ed.). American Rock Mechanics Association, Balkema: Rotterdam, 85-96*.

[20]. Koo, C. and Chern, J. (1997). Modeling of progressive fracture in jointed rock by DDA method. *In Proceedings of the Second International Conference on Analysis of Discontinuous Deformation, Ohnishi Y (ed.). Japan Institute of Systems Research: Kyoto, 186-201*.

[21]. Amadei, B., Lin, C., and Dewyer, J. (1996). Recent extensions to DDA. *In: Salami, M.R. & Banks, D. (eds.) First International Forum on Discontinuous Deformation Analysis and Simulations of Discontinuous Media. Berkeley, CA: TSI Press*.

[22]. Lin, C., Amadei, B., Ouyang, S., and Huang, C. (1995). Development of fracturing algorithms for jointed rock masses with the discontinuous deformation analysis. *In: Li, J.C., Wang, C.-Y., and Sheng, J. (eds.) The First International Conference on Analysis of Discontinuous Deformation, Changli, 64-90*.

[23]. Ma, Y., Jiang, W., Huang, Z., and Zheng, H. (2007). A new meshfree displacement approximation mode for DDA method and its application. *In: Ju, Y., Fang, X., and Bian, H. (eds.) The Eighth International Symposium on Analysis of Discontinuous Deformation, Beijing, 81-88*.

[24]. Bao, H. and Zhao, Z. (2010). Modelling crack propagation with nodal-based discontinuous deformation analysis. *In: Ma, G. and Zhou, Y. (eds.) Analysis of Discontinuous Deformation: New Developments and Applications. Singapore, 161–167*.

[25]. Ben, Y., Wang, Y., and Shi, G. (2013). Development of a model for simulating hydraulic fracturing with DDA. *In: Proceedings of the 11th International Conference on Analysis of Discontinuous Deformation (ICADD'13), 169–175*.

[26]. Jiao, Y.Y., Zhang, X.L., Zhang, H.Q., and Huang, G.H. (2014). A discontinuous numerical model to simulate rock failure process. *Geomechanics and Geoengineering, 9(2), 133-141*.

[27]. Wang, C. and Wang, S. (2022). Modified Generalized Maximum Tangential Stress Criterion for Simulation of Crack Propagation and its Application in Discontinuous Deformation Analysis. *Engineering Fracture Mechanics, 259, 108-159.*

[28]. Fu, J., Haeri, H., Sarfarazi, V., Asgari, K., Ebneabbasi, P., Fatehi Marji, M., and Guo, M. (2022). Extended finite element method simulation and experimental test on failure behavior of defects under uniaxial compression. *Mechanics of Advanced Materials and Structures, 29(27), 6966-6981*.

[29]. Abdollahipour, A., Fatehi Marji, M., Yarahmadi Bafghi, A., and Gholamnejad, J. (2016). Time-dependent crack propagation in a poroelastic medium using a fully coupled hydromechanical displacement discontinuity method. *International Journal of Fracture, 199, 71-87.*

[30]. Abdollahipour, A., Fatehi Marji, M., Yarahmadi Bafghi, A., and Gholamnejad, J. (2015). Simulating the propagation of hydraulic fractures from a circular wellbore using the Displacement Discontinuity Method. *International Journal of Rock Mechanics and Mining Sciences, 80, 281-291*.

[31]. Lak, M., Fatehi Marji, M., Yarahmadi Bafghi, A., and Abdollahipour, A. (2019a). Analytical and numerical modeling of rock blasting operations using a two-dimensional elasto-dynamic Green's function. *International Journal of Rock Mechanics and Mining Sciences, 114, 208-217.*

[32]. Crouch, S. (1976). Solution of plane elasticity problems by the displacement discontinuity method. I. Infinite body solution. *International Journal for Numerical Methods in Engineering, 10(2), 301-343.*

[33]. Shi, G.h. (1988). Discontinuous Deformation Analysis – A New Numerical Model for the Static and Dynamics of Block Systems. *PhD Dissertation, University of California, Department of Civil Engineering, Berkeley*.

[34]. Crouch, S. and Starfield, A. (1983). Boundary Element Methods in Solid Mechanics. *London: George Allen & Unwin Press*.

[35] Haeri, H., Khaloo, A., Shahriar, K., Fatehi Marji, M., and Moaref vand, P. (2015). A boundary element analysis of crack-propagation mechanism of micro-cracks in rock-like specimens under a uniform normal tension. *Journal of Mining and Environment, 6(1), 73-93*.

[36]. Fatehi Marji, M., Hosseini_Nasab, H., and Kohsary, A. (2006). On the uses of special crack tip elements in numerical rock fracture mechanics. *International Journal of Solids and Structures, 43(6), 1669-1692*.

[37]. Duran, O., Sanei, M., Devloo, P.R.B., and Santos, E.S.R. (2020). An enhanced sequential fully implicit scheme for reservoir geomechanics. *Comput Geosci 24(4): 1557–1587*.

[38]. Sanei, M., Durán, O., Devloo, P.R.B., and Santos, E.S.R. (2021). Analysis of pore collapse and shear-enhanced compaction in hydrocarbon reservoirs using coupled poro-elastoplasticity and permeability. *Arab J Geosci*.

[39]. Sanei, M., Durán, O., Devloo, P.R.B., and Santos, E.S.R. (2022). Evaluation of the impact of strain-dependent permeability on reservoir productivity using iterative coupled reservoir geomechanical modeling. *Geomech Geophy Geo Energy Geo Res*.

[40]. Haeri, H., Shahriar, K., Fatehi Marji, M., and Moarefvand, P. (2014a). On the Strength and Crack Propagation Process of the Pre-Cracked Rock-like Specimens under Uniaxial Compression. *Strength of Materials, 46, 140-152.*

[41]. Wong R H C, Tang C A, Chau K T, Lin P. (2002). Splitting failure in brittle rocks containing pre-existing flaws under uniaxial compression. *Engin Frac Mecha, 69: 1853−1871*.

[42]. Yang, W., Zhang, Q., P.G, R, Yu, R., Luo, G., Chenchen, H., and Wang, G. (2019). A damage mechanical model applied to the the analysis of mechanical properties of jointed rock masses. *Tunnelling and Underground Space Technology, 84, 113-128.*

[43]. Zhao, Z., An, X., and Zhou, Y. (2013). DDA/NMM developments and applications in Nanyang Technological University, Singapore. *In: Chen, G., Ohnishi, Y., Zheng, L., and Sasaki, T. (eds.) The 11th International Symposium on Analysis of Discontinuous Deformation, 67-80*.

[44]. Haeri, H., Shahriar, K., Fatehi Marji, M., and Moaref vand, P. (2014b). Cracks coalescence mechanism and cracks propagation paths in rock-like specimens containing pre-existing random cracks under compression. *J. Cent. South Univ., 21, 2404-2414*.

کوپل آنالیز تغییرشکل ناپیوسته (DDA) و روش ناپیوستگی جابجایی (DDM) برای شبیه‌سازی مکانیزم شکست در ژئومتریال

محسن خانی زاده بهابادی[1*]، علیرضا یاراحمدی بافقی[1]، محمد فاتحی مرجی[1]، حسین شهامی[1] و ابوالفضل عبداللهی پور[2]

۱. بخش مهندسی معدن، دانشگاه یزد، ایران

۲. بخش مهندسی ژئومکانیک نفت، دانشگاه تهران، ایران

ارسال ۲۰۲۳/۰۸/۳۰، پذیرش ۲۰۲۳/۱۲/۳۰

* نویسنده مسئول مکاتبات: m_khani_bahabadi@yahoo.com

چکیده:

پیچیدگی رفتار ژئومتریال فراتر از توانایی روش‌های عددی مرسوم است که به تنهایی برای مدلسازی واقعی سازه‌های سنگی استفاده شود. کوپل روش‌های عددی می‌تواند مدلسازی عددی را واقعی‌تر کند. روش آنالیز تغییرشکل ناپیوسته (DDA) و ناپیوستگی جابجایی (DDM) برای مدلسازی مکانیزم جابجایی بلوک و انتشار ترک در توده سنگ بلوکی ترکیب شده است. DDA برای محاسبه جابجایی‌های بلوک‌ها استفاده شده و DDM برای پیش‌بینی مسیر انتشار ترک ناشی از شرایط مرزی تعیین شده، مورد استفاده قرار گرفته شده است. جابجایی‌های بدست آمده از DDA به تنش تبدیل شده و با توجه به راه‌حل کلوین، مسئله مکانیزم انتشار ترک در داخل هر بلوک بررسی می‌گردد. تنش‌های مرزی بدلیل انتشار ترک بروزرسانی شده و بعنوان شرایط جدید تنش مرزی در DDA اعمال می‌شود. این چرخه تا زمانی که انتشار ترک متوقف شود یا بلوک جدید تشکیل گردد، ادامه خواهد داشت. حل عددی نمونه‌های سنگی آزمایشگاهی شامل نمونه‌هایی که شامل دو ترک تصادفی که ترک ۱ ثابت شده و ترک ۲ با زوایای مختلف ایجاد شده و نمونه‌ای شامل یک ترک با زاویه شیب ۳۰ درجه با نتایج عددی و آزمایشگاهی موجود مقایسه شده است. این مقایسه دقت و اثربخشی روش پیشنهادی را تأیید می‌کند زیرا مسیرهای انتشار ترک پیش‌بینی شده با نتایج تجربی مربوطه نمونه‌های سنگ مطابقت دارد.

کلمات کلیدی: ژئومتریال، آنالیز تغییرشکل ناپیوسته، روش ناپیوستگی جابجایی، انتشار ترک، کوپل روش‌های عددی.